PNNL-34123 Rev 0
EWG-RPT-042 Rev 0

Product Consistency Test and Vapor Hydration Test Comparisons of a Radioactive Hanford Waste Glass with its Non-Radioactive Simulant Glass

April 2023

JT Reiser
JJ Neeway
B Parruzot
EA Cordova
SK Cooley
JD Vienna

U.S. DEPARTMENT OF ENERGY
Prepared for the U.S. Department of Energy
under Contract DE-AC05-76RL01830

PACIFIC NORTHWEST NATIONAL LABORATORY
operated by
BATTELLE
for the
UNITED STATES DEPARTMENT OF ENERGY
under Contract DE-AC05-76RL01830

Printed in the United States of America

Available to DOE and DOE contractors from the
Office of Scientific and Technical Information,
P.O. Box 62, Oak Ridge, TN 37831-0062;
ph: (865) 576-8401
fax: (865) 576-5728
email: reports@adonis.osti.gov

Available to the public from the National Technical Information Service
5301 Shawnee Rd., Alexandria, VA 22312
ph: (800) 553-NTIS (6847)
email: orders@ntis.gov <https://www.ntis.gov/about>
Online ordering: http://www.ntis.gov

PNNL-34123 Rev 0
EWG-RPT-042 Rev 0

Product Consistency Test and Vapor Hydration Test Comparisons of a Radioactive Hanford Waste Glass with its Non-Radioactive Simulant Glass

April 2023

JT Reiser
JJ Neeway
B Parruzot
EA Cordova
SK Cooley
JD Vienna

Prepared for
the U.S. Department of Energy
under Contract DE-AC05-76RL01830

Pacific Northwest National Laboratory
Richland, Washington 99354

Summary

Product Consistency Tests (PCT) and Vapor Hydration Tests (VHT) were performed on a radioactive glass made from Hanford tank AP-107 waste (i.e., R-AP-107) and its non-radioactive equivalent glass made from simulated tank waste (i.e., S-AP-107). The radioactive and non-radioactive experiments were conducted in parallel with identical equipment, protocols, and staff to remove additional experimental uncertainties. PCT and VHT results are reported for all samples and are shown in Table S.1. Average normalized mass loss of B (NL_B) and Na (NL_{Na}) calculated from the three replicate test results for each glass with their respective standard deviations (*SD*) are presented for PCT results while individual VHT rates (r_{VHT}) with their propagated errors ($\sigma_{r_{prop}}$) from individual thickness measurements on each sample are presented for the VHT results. Some VHT samples experienced more than 50% evaporation loss during the experiments. However, no visible alteration was detected on any VHT samples regardless on the amount of evaporation loss detected as shown in Table S.1.

Table S.1. Average NL_B and NL_{Na} and standard deviations for the three replicates of R-AP-107 and S-AP-107, and individual VHT rates (r_{VHT}) with propagated errors ($\sigma_{r_{prop}}$) from individual thickness measurements. The DOE limits for NL_B, NL_{Na}, and r_{VHT} are provided for comparison.

	R-AP-107	**S-AP-107**
Average NL_B ± SD (g·m^{-2})	0.51 ± 0.05	0.37 ± 0.01
Average NL_{Na} ± SD (g·m^{-2})	0.61 ± 0.04	0.42 ± 0.01
NL_B and NL_{Na} DOE Limits (g·m^{-2})	2	2
VHT Replicate 1: $r_{VHT} \pm \sigma_{r_{prop}}$ (g m^{-2} d^{-1})	3 ± 5	-1 ± 3
VHT Replicate 2: $r_{VHT} \pm \sigma_{r_{prop}}$ (g m^{-2} d^{-1})	2 ± 4	0 ± 3
VHT Replicate 3: $r_{VHT} \pm \sigma_{r_{prop}}$ (g m^{-2} d^{-1})	4 ± 7	3 ± 8
r_{VHT} DOE limit	50	50
Underlined values indicate the test had more than 50% evaporation loss		

Statistical analyses were performed on the results and indicated that the test responses were within experimental uncertainty for all PCT and VHT experiments. The experimental uncertainties were estimated using pooled standard deviations determined in Vienna et al. (2022) which incorporated estimates of SDs from several replicate sets of other low-activity waste (LAW) glasses to include uncertainties due to fabricating glasses, performing experiments, and sample measurements (e.g., leachate analysis). The pooled standard deviations are a better representation than simple SD determined from three replicates for one glass. Statistical analysis was also performed using simple SD and propagated errors for the VHT samples for comparison. The VHT samples were still within experimental uncertainty regardless of how the experimental uncertainty was represented. These results help to confirm the Waste Treatment and Immobilization Plant composition control methods that predict PCT and VHT responses using models fit primarily to non-radioactive simulant glasses are valid for radioactive tank waste glasses.

Acknowledgments

The authors gratefully acknowledge the financial support provided by the U.S. Department of Energy Office of River Protection Waste Treatment and Immobilization Plant Project managed by Tom Fletcher, with technical oversight by Albert Kruger. The authors thank the staff in the Environmental Sciences Laboratory at Pacific Northwest National Laboratory for solution analysis. The following Pacific Northwest National Laboratory staff members are acknowledged for their contributions: Derek Dixon, Derek Cutforth, and Steven Luksic for laboratory assistance, David MacPherson for quality assurance, and Chrissy Charron, Cassie Martin, Will Eaton, and Renee Russell for programmatic support during the conduct of this work.

Acronyms and Abbreviations

DIW	deionized water
DOE	U.S. Department of Energy
DWPF	Defense Waste Processing Facility
GFA	glass formulation algorithm
GFC	glass forming chemical
HLW	high-level waste
ICP-OES	inductively coupled plasma–optical emission spectroscopy
ICP-MS	inductively coupled plasma-mass spectrometry
IDF	Integrated Disposal Facility
IHLW	immobilized high-level waste
ILAW	immobilized low-activity waste
LAW	low-activity waste
NQAP	Nuclear Quality Assurance Program
ORP	DOE Office of River Protection
PCT	Product Consistency Test
PNNL	Pacific Northwest National Laboratory
QA	quality assurance
RPD	relative percent differences
VHT	Vapor Hydration Test
wt%	weight percent
WTP	Waste Treatment and Immobilization Plant

Contents

Figures

Tables

1.0 Introduction

The U.S. Department of Energy (DOE) Office of River Protection (ORP) is responsible for the safe storage, treatment and immobilization of the Hanford Site tank wastes. The Hanford Waste Treatment and Immobilization Plant (WTP) is being built to provide DOE with a capability to treat the waste by vitrification for subsequent disposal. The tank waste will be partitioned into low-activity waste (LAW) and high-level waste (HLW) fractions, which will then be vitrified, respectively, into immobilized low-activity waste (ILAW) and immobilized high-level waste (IHLW) products. The ILAW product will be disposed of in the Integrated Disposal Facility (IDF) on the Hanford Site, while the IHLW product will be temporarily stored on-site prior to disposal at a national deep geological disposal facility for high-level nuclear waste.

The ILAW products must satisfy a variety of requirements with respect to regulatory compliance and protection of the environment before they can be accepted for disposal. The WTP Contract specifies that the responses of ILAW to the Product Consistency Test (PCT, ASTM C1285) and Vapor Hydration Test (VHT, ASTM C1663) must satisfy numerical constraints (DOE 2000) where DOE states the following:

"2.2.2.17.2 Product Consistency Test: The normalized mass loss of sodium, silicon, and boron shall be measured using a seven-day product consistency test run at 90 °C as defined in ASTM C1285-98. The test shall be conducted with a glass to water ratio of 1 gram of glass (-100 +200 mesh) per 10 milliliters of water. The normalized mass loss shall be less than 2.0 grams/m^2. Qualification testing shall include glass samples subjected to representative waste form cooling curves. The product consistency test shall be conducted on waste form samples that are statistically representative of the production glass.

2.2.2.17.3 Vapor Hydration Test: The glass corrosion rate shall be measured using at least a seven (7)-day vapor hydration test run at 200 °C as defined in the DOE-concurred upon ILAW Product Compliance Plan. The measured glass alteration rate shall be less than 50 grams/(m^2 day). Qualification testing shall include glass samples subjected to representative waste form cooling curves. The vapor hydration test shall be conducted on waste form samples that are representative of the production glass."[1]

A vast majority of all ILAW glass durability data generated to-date is based on simulated waste glasses fabricated using crucible melts. PCT data have been generated for six glasses fabricated at crucible scale with radioactive Hanford LAW and their respective non-radioactive glasses made from simulant waste (Figure 1.1, Vienna (2004)). All sample pairs except one were found to have relative percent differences (RPD) less than or equal to experimental uncertainty which includes errors due to sample preparation, instrument variances, and random errors. The one exception, the AN-102 glass pair, measured RPD of roughly double the experimental uncertainty (indicated by solid symbols in Figure 1.1).

[1]For this work, ASTM C1285-21 was used instead of ASTM C1285-98 which is an updated version of ASTM C1285-98. There are no major changes between the procedures described in the two versions.

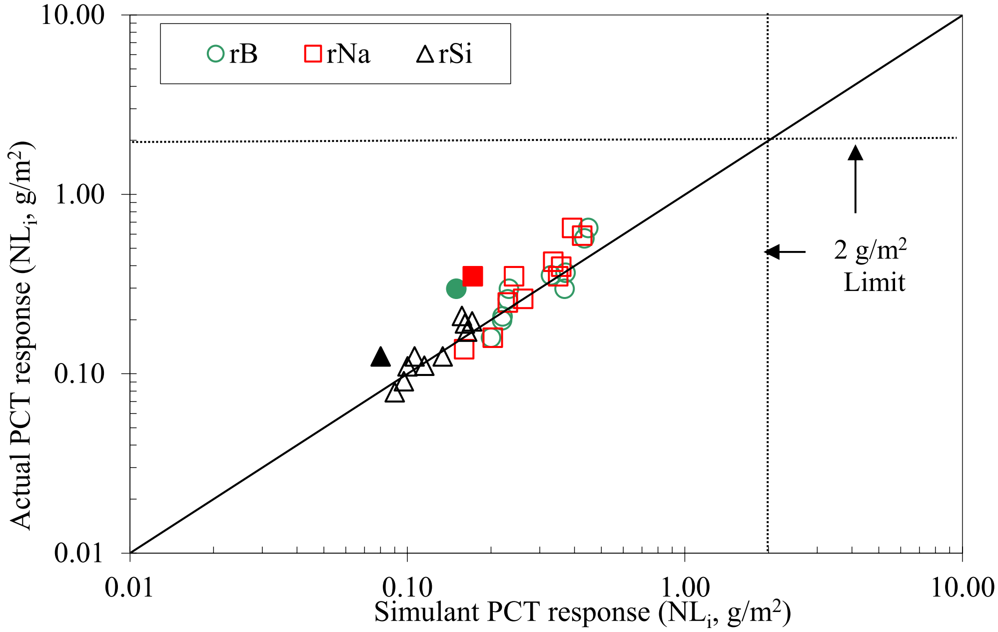

Figure 1.1. Comparison of PCT responses (normalized loss, NL_i, $g \cdot m^2$) for radioactive actual and non-radioactive simulated LAW glasses. The solid symbols represent AN-102 PCT responses discussed in the text. (Vienna. 2004)

No VHT experiments have been performed to date on glasses fabricated with actual WTP LAW. VHT is a notoriously noisy test with repeat measurements being on the order of 63 RPD for simulant glasses only.

The purpose of this task is to perform PCT and VHT on glasses fabricated using Hanford LAW and its simulant in laboratory-scaled melters to evaluate differences in their responses. This report presents the PCT and VHT data of an actual radioactive waste glass and its respective non-radioactive simulant glass and statistical analysis calculations to determine if the differences between measured PCT and VHT responses of actual and simulated waste glasses are statistically significant.

2.0 Quality Assurance

This work was performed in accordance with the Pacific Northwest National Laboratory (PNNL) Nuclear Quality Assurance Program (NQAP). The NQAP complies with DOE Order 414.1D, *Quality Assurance*, and 10 CFR 830, *Nuclear Safety Management*, Subpart A, *Quality Assurance Requirements*. NQAP uses NQA-1-2012, *Quality Assurance Requirements for Nuclear Facility Application*, as its consensus standard and NQA-1-2012, Subpart 4.2.1, as the basis for its graded approach to quality.

The NQAP works in conjunction with PNNL's laboratory-level Quality Management Program, which is based on the requirements as defined in DOE Order 414.1D and 10 CFR 830 Subpart A.

The work of this report was performed to the quality assurance (QA) level of applied research with a technology readiness level (TRL) of 8.

3.0 Test Methods

3.1 Glass Selection

Previous tasks at PNNL have generated glasses from radioactive and non-radioactive continuous laboratory-scaled melters, which are already available for durability tests. Glasses made from AP-107 tank waste (i.e., “AP-107-1R”) and an AP-107 simulant (i.e., “AP107WDFL”) from Dixon et al. (2020) were chosen to be tested in parallel for their PCT and VHT responses. For the present study, the glasses were renamed for clarity: radioactive glass “AP-107-1R” was renamed to “R-AP-107 and simulant glass “AP107WDFL” was renamed to “S-AP-107”. The target compositions of R-AP-107 and S-AP-107 are provided in Table 3.1 (minus the minor elements), which shows the two glasses are similar.

During a melter session, glass is produced during multiple pours which lead to slight variations in glass composition from pour-to-pour. The measured compositions of the R-AP-107 and S-AP-107 are presented in Table 3.2which provide concentrations of the major and minor elements of the specific glass pour of the respective glasses used for PCT and VHT. The R-AP-107 measured composition is the “Sample Glass Pour 9.42” in Dixon et al. (2020) was not analyzed for minor radioisotopes (i.e., Np-237, Cm-242, Cm-243/Cm-244, Am-241, Pu-238, Pu-239/Pu-240). The measured compositions confirm the R-AP-107 and S-AP-107 glasses are similar (<12 RPD for components with >1 wt% in glass except for Li and Ca). R-AP-107 contains nearly 90% more Li and 25% more Ca than S-AP-107. Higher concentrations of Li_2O are known to increase both PCT and VHT responses while increasing CaO concentrations has a smaller and mixed effect on PCT and VHT (Vienna et al. 2022, Table 9.3).

Table 3.1. Target compositions (wt %) for R-AP-107 and S-AP-107 from Dixon et al. (2020).

	Target, wt %	
Component	**R-AP-107**	**S-AP-107**
Al_2O_3	6.13	6.10
B_2O_3	9.95	10
CaO	4.53	3.94
Cr_2O_3	0.07	0.08
Fe_2O_3	5.52	5.5
K_2O	0.36	0.38
Li_2O	1.52	0.89
MgO	1.49	1.48
Na_2O	16.34	17.2
NiO	0.01	0
SiO_2	45.36	45.5
TiO_2	1.4	1.4
ZnO	3.51	3.5
ZrO_2	3.02	3
Cl	0.18	0.42
F	0.03	0.04
P_2O_5	0.19	0.13
SO_3	0.39	0.44

Table 3.2. Target compositions (wt %) and measured compositions (ppm) for R-AP-107 and S-AP-107. The R-AP-107 composition is from Dixon et al. (2020). Not measured results are represented by "NM".

	Measured, ppm	
Component	**R-AP-107**	**S-AP-107**
Al	31400	30700
B	30100	30000
Ba	37.7	112
Ca	31600	25600
Cd	4.75	6.32
Cr	885	837
Cs	4.03	NM
Co	3.8	7.03
Cu	18.1	17.2
Fe	37100	41700
K	3100	3110
La	2.51	575
Pb	5.01	32.2
Li	6520	3480
Mg	8550	8680
Mn	87.7	98.2
Mo	47.7	205
Na	125000	125000
Ni	163	323
Si	213000	215000
Sr	36.5	87.3
Tc	2.24	NM
Ti	8410	8860
Zn	28400	27200
Zr	20400	20300
Cl	NM	2439.6
F	434	141.9
P	628	742
S	1570	1690
Sn	24.3	18
Re	NM	4.37
W	247	196
V	54.4	60.1
Y	39.3	41.5

3.2 Experimental Considerations

PNNL has previously performed hundreds of durability tests on non-radioactive simulant glasses. However, the existing laboratory spaces where these previous tests were performed are not equipped to handle radioactive samples. Thus, additional laboratory space and equipment were obtained, but various lab procedures and equipment were modified based on safety needs and availability. Therefore, R-AP-107 and S-AP-107 were prepared with the same (or identical) equipment and procedures.

The following nomenclature is used for experiment names throughout the text:

Sample ID = Batch ID-AAA-X

Where:

Batch ID = Glass name (e.g., R-AP-107, S-AP-107)

AAA = Test method (i.e., PCT, VHT)

X = Replicate ID (e.g., a, b, or c)

3.3 Product Consistency Test

PCT experiments were performed in triplicate for R-AP-107 and S-AP-107 using Method A of the standard ASTM International procedure *Standard Test Methods for Determining Chemical Durability of Nuclear, Hazardous, and Mixed Waste Glasses and Multiphase Glass Ceramics: The Product Consistency Test (PCT)* (ASTM C1285-21). Approved reference material – 1 (ARM-1) glass was tested concurrently with the samples as a reference material since it had previously been tested in a multi-laboratory round robin (Ebert 2019). The composition of ARM-1 is given in Appendix A. All glass samples were crushed, sieved to an aperture size of 75 – 150 µm (200 and 100 mesh, respectively), and washed according to ASTM C1285-21. The prepared glass was added to ASTM Type 1 18.2 MΩ·cm deionized water (DIW, ASTM D1193-06R18) in a 1.2 g:12 mL ratio in Type 304L stainless steel vessels cleaned according to ASTM C1285-21. The vessels were closed, tightened, and placed into an oven at 90 °C ± 2 °C for 7 days ± 3 hours (i.e., ± 2% test duration). After 7 days, the vessels were removed from the 90 °C ± 2 °C oven and cooled to room temperature. Final vessel masses and solution pH at room temperature (pH_{RT}) were recorded. Approximately 2 mL of leachate solution was passed through a 0.45-µm filter and acidified with ~8 mL of 2 wt% HNO_3. The acidified solutions were analyzed by inductive coupled plasma optical emission spectroscopy (ICP-OES) for B, Na, and Si for all samples and by inductive coupled plasma mass spectrometry (ICP-MS) for Tc in the R-AP-107 samples and blanks.

Normalized concentrations for element *i* (NC_i, g·L^{-1}) were calculated according to Equation 3.1.

$$NC_i = \frac{C_i}{f_i} \tag{3.1}$$

where: C_i = concentration of element *i* in the leachate solution in the test vessel (g·L^{-1})
f_i = mass fraction of element *i* measured in the unaltered glass (See Appendix A, Table A.2).

Additionally, normalized mass losses for element *i* (NL_i, g·m^{-2}) was calculated according to Equation 3.2.

$$NL_i = \frac{NC_i}{(SA/V)} \tag{3.2}$$

where: SA = surface area of the glass (m^2)
V = volume of solution (L).

SA is estimated from the mean sieve aperture size via Equation 3.3 as follows:

$$SA = \frac{6m}{\rho d} \cdot \left(\frac{1\,meter}{100\,centimeters}\right)^2 = \frac{3m}{\rho r} \cdot \left(\frac{1\,meter}{100\,centimeters}\right)^2 \tag{3.3}$$

where: m = initial mass of glass (g)
ρ = density of the glass ($g{\cdot}cm^{-3}$)
d = average particle diameter, 112.5 µm
r = average particle radius, 56.25 µm

The densities, ρ, used for the R-AP-107 and S-AP-107 were 2.66 $g{\cdot}cm^{-3}$ which is the average density for LAW glasses provided in Muller et al. (2001) and Rielley et al. (2001). The density for ARM-1 is 2.75 $g{\cdot}cm^{-3}$ from Ebert (2019).

Results are reported in Section 4.1.

3.4 Vapor Hydration Test

For Vapor Hydration Tests (VHT), monolith glass samples were altered in water vapor at 200 °C in sealed stainless-steel vessels according to the ASTM International standard procedure *Standard Test Method for Measuring Waste Glass or Glass Ceramic Durability by Vapor Hydration Test* (ASTM C1663-18). Due to the safety protocols specified for radioactive work, some steps in ASTM C1663-18 were modified.

Select glass pieces were annealed at 500 °C for one hour and then cooled naturally overnight to <50 °C at which point they were removed from the oven. Monoliths with approximate dimensions of 2 mm × 10 mm × 10 mm samples were cut from the annealed glasses using a water lubricated diamond-impregnated saw. Typically, all six sides of the monoliths are polished by hand to 1.5 mm × 10 mm × 10 mm at 600 grit. For this work, no direct hand contact was allowed while polishing due to the risk of laceration through the gloves and skin, which would result in internal exposure to radioactivity. Instead, the coupons were mounted on aluminum pucks, as shown in Figure 3.1, and polished through successive steps to 600 grit on only the two large faces. Each final dimension was measured in three locations by calipers, and the average and standard deviations for each dimension were calculated. The average initial dimensions and their standard deviations are given in Table B.1 in Appendix B and were approximately 1.5 mm × 10 mm × 10 mm for each coupon.

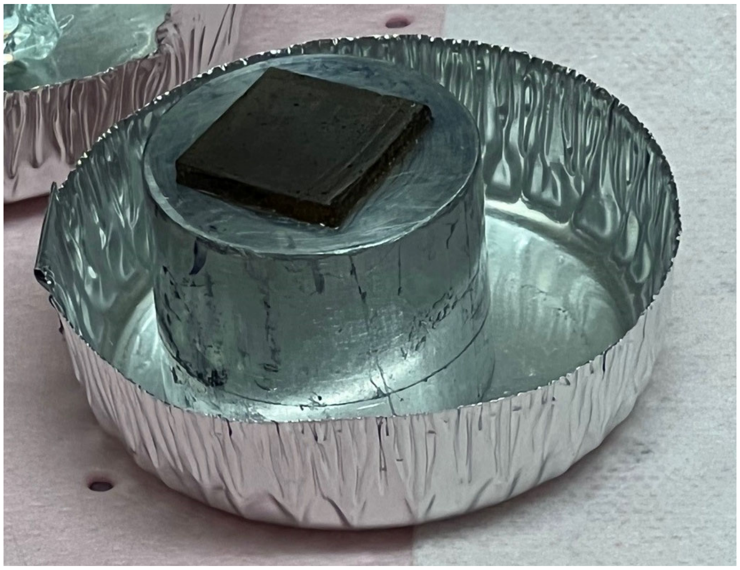

Figure 3.1. Example of a mounted unpolished VHT monolith sample

The polished samples were secured with Pt wire from stainless-steel supports within stainless-steel vessels. DIW was added to the bottom of the vessels so that enough DIW was present to react with the specimens in the vapor state but not enough to reflux during testing (~0.20 g). The vessels were closed and tightened to 20.3 – 23.0 N·m (i.e., 15.0 – 17.0 ft·lb) and then placed in a convection oven preheated to 200 ± 2 °C for 24 days.

After 24 days, the vessels were removed from the oven, weighed, and then quenched in water. The altered VHT monoliths were removed from the vessels, and the pH_{RT} of the remaining solutions were measured with pH paper. ASTM C1663-18 specifies that a post-experiment solution pH >10 may signify reflux conditions in the vessel, indicating the experimental results may need to be repeated. Additionally, ASTM C1663-18 indicates that experiments with >50% evaporation loss may also need to be repeated.

The post-VHT monoliths were air dried, mounted in epoxy, crossed-sectioned, and polished to 600 grit for analysis by optical microscopy-image analysis to determine the amount of remaining unaltered glass after the VHT experiments. Examples of cross sections of post-VHT monoliths are provided in Figure 3.2. Individual and average remaining glass thicknesses are provided in Table B.2 in Appendix B.

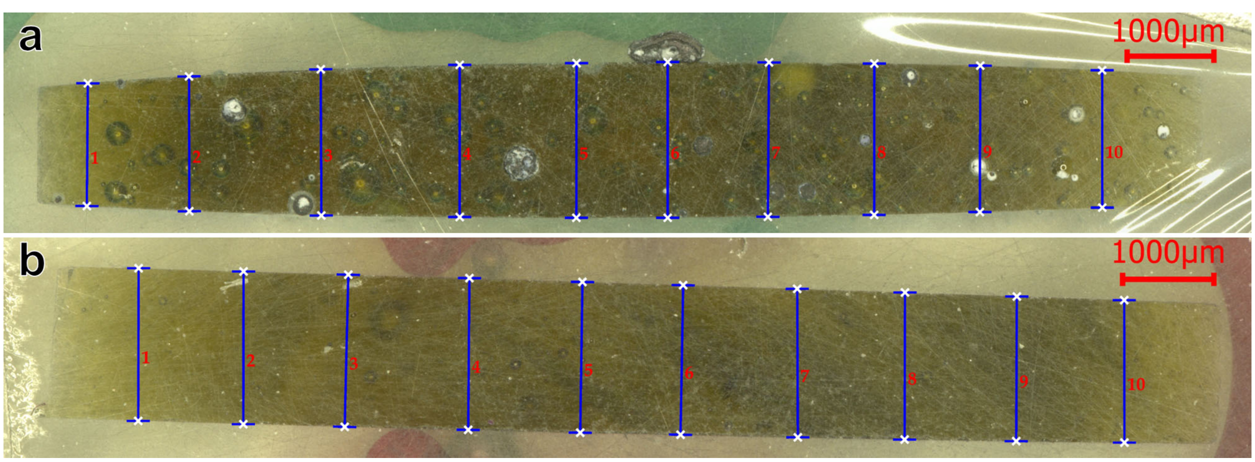

Figure 3.2. Examples of VHT cross section measurements: a) R-AP-107-VHT-c and b) S-AP-107-VHT-a.

The remaining glass thicknesses of the monoliths were determined by performing 10 measurements distributed across the cross section of the sample (see Figure 3.2). Then, the average and standard deviation of the 10 remaining glass thickness measurements were calculated. The individual remaining glass thickness measurements, averages, and standard deviations are provided in Appendix A. The amount of glass altered per unit surface area of specimen (m_a, g·mm^{-2}) was determined from the average thickness of remaining glass according to Equation 3.4 from ASTM C1663-18, Equation 6:

$$m_a = \frac{m_i}{2 \cdot w_i \cdot l_i} \cdot \left(1 - \frac{d_r}{d_i}\right) \tag{3.4}$$

where: m_i = initial glass monolith mass (g); treated as a constant for error propagation as only one mass measurement was made.

w_i = average initial glass monolith width (mm)
l_i = average initial glass monolith length (mm)
d_i = average initial thickness of the glass monolith (mm)
d_r = average thickness of remaining glass (mm)

Error propagation of m_a (σ_{m_a}) was determined by applying the general formula for uncertainty of a general function (ASTM C1663-18, equation 8) to yield Equation 3.5:

$$\sigma_{m_a} = m_a \cdot \sqrt{\left(\frac{\sigma_{w_i}}{w_i}\right)^2 + \left(\frac{\sigma_{l_i}}{l_i}\right)^2 + \left(\frac{\sigma_{d_r/d_i}}{1 - d_r/d_i}\right)^2} \tag{3.5}$$

where: σ_{w_i} = initial glass width standard deviation (mm)
σ_{l_i} = initial glass length standard deviation (mm)
σ_{d_r/d_i} = propagated error for d_r/d_i as defined in Equation 3.6 below:

$$\sigma_{d_r/d_i} = \frac{d_r}{d_i} \cdot \sqrt{\left(\frac{\sigma_{d_r}}{d_r}\right)^2 + \left(\frac{\sigma_{d_i}}{d_i}\right)^2} \tag{3.6}$$

where: σ_{d_i} = initial glass thickness standard deviation (mm)
σ_{d_r} = remaining glass thickness standard deviation (mm).

Individual rates of VHT corrosion (r_{VHT}, g·m^{-2}·d^{-1}) for each sample were determined via Equation 3.7:

$$r_{VHT} = \frac{m_a}{t} \cdot \left(\frac{1000\ millimeter}{1\ meters}\right)^2 \tag{3.7}$$

where: t = test duration (d).

Error propagation for individual r_{VHT} values ($\sigma_{r_{prop}}$, g·m^{-2}·d^{-1}) was calculated using Equation 3.8 which assumed no error in t:

$$\sigma_{r_{prop}} = \frac{\sigma_{m_a}}{t} \cdot \left(\frac{1000\ millimeter}{1\ meter}\right)^2 \tag{3.8}$$

The ln[r_{VHT}] values were determined for all individual samples. Propagated errors for ln[r_{VHT}] values ($\sigma_{\ln[r_{prop}]}$) were determined by Equation 3.9 which was derived by the general formula for uncertainty of a general function (ASTM C1663-18, Equation 8) as follows:

$$\sigma_{\ln[r_{prop}]} = \frac{\sigma_{r_{prop}}}{r_{VHT}} \quad (3.9).$$

Average ln[r_{VHT}] values ($\overline{\ln[r_{VHT}]}$) for each glass were calculated from individual replicate ln[r_{VHT}] values for each glass. Errors for $\overline{\ln[r_{VHT}]}$ were calculated using two approaches: 1) a simple standard deviation ($SD_{\ln[r_{VHT}]}$) for the individual ln[r_{VHT}] which ignores the propagated errors determined from the 10 measurements performed on each sample, and 2) a combined uncertainty of the individual $\sigma_{\ln[r_{prop}]}$ values ($\bar{\sigma}_{\ln[r_{prop}]}$) as shown in Equation 3.10:

$$\bar{\sigma}_{\ln[r_{prop}]} = \frac{\sqrt{\sum_j \sigma_{\ln[r_{prop}]}}}{j} \quad (3.10)$$

where: j = the number of replicate tests for each glass.

3.5 Test Statistic Calculations

Test statistic calculations and p-values were determined using PCT and VHT results. Individual calculations are described in Sections 4.1.2 and 4.2.2, but a general discussion of the calculations is described here.

The t-statistic or z-statistic values that are often used as the test statistic, or as the form of the basis of confidence interval formulas, follow the general formula in Equation 3.11:

$$test\ statistic = \frac{\hat{\theta} - \theta_0}{SE(\hat{\theta})} \quad (3.11)$$

where: $\hat{\theta}$ = an estimator of a parameter of interest, θ, typically derived from sample data
θ_0 = the hypothesized value of θ
$SE(\hat{\theta})$ = the standard error (uncertainty estimate) associated with $\hat{\theta}$, typically derived from the same sample data that produced $\hat{\theta}$.

The calculated test statistic is generally referred to as a z-statistic in cases where sample size is sufficiently large (i.e., the t-distribution approaches a z-distribution or normal distribution as sample size increases) or when the uncertainty inputs are known rather than being estimates from sample data (which is rarely the case). Alternatively, t-statistics are used for limited sample sizes.

For the test statistics in this study, the parameter of interest is the difference between R-AP-107 and S-AP-107 PCT or VHT responses. The null hypothesis for the tests is that the difference is zero.

Equation 3.11 was tailored to calculated t-statistic values for VHT data using simple standard deviations as uncertainties. The other test statistic calculations use z-statistic approach adaptions of Equation 3.11 for PCT and VHT data where uncertainty estimates are obtained from other sources rather from direct calculations using the sample data that produced the parameter estimate (e.g., propagated errors, pooled standard deviations). The details of these calculations are described in Sections 4.1.2 and 4.2.2.

Additionally, respective *P-values* for the 90% confidence interval were calculated from each test statistic. The *P-value* is a statistical test that examines the probability of a null hypothesis being correct. In this case, the *P-value* evaluates the probability that the PCT or VHT responses of two samples (e.g., R-AP-107 and S-AP-107) are not statistically different. A high *P-value* indicates the responses are not statistically different – where the commonly used thresholds for significant differences are 0.05 or 0.10 (corresponding to 95% and 90 % confidence intervals, respectively). Thus, *P-values* >0.10 suggest the durability responses are not statistically different.

4.0 Results and Discussion

4.1 Product Consistency Test

4.1.1 PCT Results

The individual and average normalized concentrations (NC_i, g·L^{-1}), normalized mass losses (NL_i, g·m^{-2}), and ln[NL_i, g·m^{-2}] for B, Na, Si, and Tc are reported in Table 4.1, Table 4.2, and Table 4.3, respectively, for R-AP-107 and S-AP-107. Standard deviations (SD) for NC_i, NL_i, and pH_{RT} were also calculated and provided in Table 4.1 and Table 4.2. No B, Na, Si and Tc were detected in any of the blank tests. Per the WTP contract (DOE 2000), NL_i values for B, Na, and Si must be below 2.0 g m^{-2}. Both glasses comply with this limit for all analyzed elements. The Tc values are congruent with the B and Na values for R-AP-107, which was also observed in MCC-1 like experiments on glasses doped with Tc-99 by Bibler and Jurgensen (1987).

Table 4.2 also contains the final pH_{RT} values measured for each replicate. In general, R-AP-107 had larger pH_{RT}, NC_i, and NL_i values than S-AP-107. These observations are likely due to the small compositional differences between the glasses, specifically the higher concentrations of Li in R-AP-107 as noted in Section 3.1. Section 4.1.2 explores the apparent differences in ln(NL_i) more thoroughly to determine whether the observed differences are within experimental uncertainty.

Table 4.1. Individual and average normalized concentrations (NC_i) for R-AP-107 and S-AP-107. Standard deviations (SD) are also provided. Not applicable results are represented by “NA”.

Sample ID	NC_B (g·L^{-1})	NC_{Na} (g·L^{-1})	NC_{Si} (g·L^{-1})	NC_{Tc} (g·L^{-1})
R-AP-107-PCT-A	0.94	1.15	0.38	1.08
R-AP-107-PCT-B	1.00	1.21	0.42	1.12
R-AP-107-PCT-C	1.12	1.31	0.44	1.31
R-AP-107 Average	**1.02**	**1.22**	**0.41**	**1.17**
R-AP-107 SD	**0.10**	**0.08**	**0.03**	**0.12**
S-AP-107-PCT-A	0.75	0.86	0.35	NA
S-AP-107-PCT-B	0.74	0.84	0.34	NA
S-AP-107-PCT-C	0.73	0.84	0.34	NA
S-AP-107 Average	**0.74**	**0.85**	**0.34**	**NA**
S-AP-107 SD	**0.01**	**0.01**	**0.01**	**NA**

Table 4.2. Individual and average normalized losses (NL_i) and room temperature pH (pH_{RT}) for R-AP-107 and S-AP-107. Standard deviations (SD) are also provided. Not applicable results are represented by "NA".

Sample ID	pH_{RT}	NL_B (g·m^{-2})	NL_{Na} (g·m^{-2})	NL_{Si} (g·m^{-2})	NL_{Tc} (g·m^{-2})
R-AP-107-PCT-A	10.94	0.47	0.57	0.19	0.54
R-AP-107-PCT-B	11.15	0.50	0.60	0.21	0.56
R-AP-107-PCT-C	11.17	0.56	0.65	0.22	0.65
R-AP-107 Average	**11.09**	**0.51**	**0.61**	**0.21**	**0.59**
R-AP-107 SD	**0.13**	**0.05**	**0.04**	**0.02**	**0.06**
S-AP-107-PCT-A	10.75	0.38	0.43	0.17	NA
S-AP-107-PCT-B	10.71	0.37	0.42	0.17	NA
S-AP-107-PCT-C	10.68	0.36	0.42	0.17	NA
S-AP-107 Average	**10.71**	**0.37**	**0.42**	**0.17**	**NA**
S-AP-107 SD	**0.04**	**0.01**	**0.01**	**0.00**	**NA**

Table 4.3. Individual and average ln(NL_i, g·m^{-2}) for R-AP-107 and S-AP-107. Not applicable results are represented by "NA".

Sample ID	ln[NL_B (g·m^{-2})]	ln[NL_{Na} (g·m^{-2})]	ln[NL_{Si} (g·m^{-2})]	ln[NL_{Tc} (g·m^{-2})]
R-AP-107-PCT-A	-0.76	-0.56	-1.66	-0.62
R-AP-107-PCT-B	-0.70	-0.50	-1.57	-0.58
R-AP-107-PCT-C	-0.58	-0.43	-1.51	-0.42
R-AP-107 Average	**-0.68**	**-0.50**	**-1.58**	**-0.54**
S-AP-107-PCT-A	-0.98	-0.84	-1.74	NA
S-AP-107-PCT-B	-0.99	-0.87	-1.77	NA
S-AP-107-PCT-C	-1.01	-0.87	-1.78	NA
S-AP-107 Average	**-0.99**	**-0.86**	**-1.76**	**NA**

Individual and average NL_i responses for B, Na, and Si for the ARM-1 reference glass are reported in Table 4.4. Standard deviations (SD) of the three triplicates are also provided. Previous average NL_i responses and uncertainties determined from a round robin experiment (Ebert 2019) are provided for comparison with estimated 95% reproducibility uncertainties (1.96·S_R) between laboratory results. The average NL_B and NL_{Na} values were within the published uncertainty while the average NL_{Si} value was slightly above the tolerance. The standard deviations of the ARM-1 responses in this study were not considered in the comparison to the ARM-1 responses in Ebert (2019) as the uncertainties in Ebert (2019) included interlaboratory results whereas the results from this study include only intra-laboratory uncertainties.

Table 4.4. Individual and average normalized loss (NL_i) responses with standard deviations (SD) determined from the triplicate tests for B, Na, and Si for ARM-1 reported with previous averages and uncertainties determined from a round robin experiment (Ebert 2019). The uncertainties from Ebert (2019) are estimated 95% reproducibility uncertainties ($1.96 \cdot S_R$) between laboratory results.

Glass ID	NL_B (g·m^{-2})	NL_{Na} (g·m^{-2})	NL_{Si} (g·m^{-2})	Source
ARM-1-PCT-a	0.34	0.35	0.176	This study
ARM-1-PCT-b	0.33	0.34	0.180	This study
ARM-1-PCT-c	0.31	0.32	0.170	This study
ARM-1 Average	**0.33**	**0.34**	**0.176**	**This study**
ARM-1 SD	**0.01**	**0.02**	**0.005**	**This study**
Reported ARM-1	**0.236 ± 0.210**	**0.233 ± 0.128**	**0.136 ± 0.025**	**Ebert, 2019**

4.1.2 PCT Statistical Comparisons

Statistical analysis comparisons were performed on the average ln[NL_i, g·m^{-2}] responses for B and Na for R-AP-107 and S-AP-107. Pooled standard deviations ($SD_{i,pooled}$, i.e., the repeatability standard deviation in ASTM C1285-21) for ln[NL_B, g·m^{-2}] and ln[NL_{Na}, g·m^{-2}], (0.2317 and 0.1845, respectively) determined from Vienna et al. (2022), were used as errors for ln[NL_B, g·m^{-2}] and ln[NL_{Na}, g·m^{-2}] for R-AP-107 and S-AP-107. The $SD_{i,pooled}$ value includes uncertainties due to fabricating glasses, performing PCTs, and leachate analysis, which is a more thorough representation of the uncertainties compared to simple standard deviation of the three replicates. Figure 4.1a shows the average ln[NL_B, g·m^{-2}] and ln[NL_{Na}, g·m^{-2}] values for R-AP-107 and S-AP-107 where the error bars represent the $SD_{i,pooled}$ values. The R-AP-107 and S-AP-107 ln[NL_i, g·m^{-2}] values are within error for both B and Na.

Further statistical analysis was performed to evaluate the absolute values of the differences of ln[NL_i, g m^{-2}] between R-AP-107 and S-AP-107 to see if the differences were greater than zero within the 90% confidence interval uncertainty. The 90% confidence interval uncertainty for PCTs ($U_{90\%\ CI,\ PCT}$) was calculated using Equation 4.1:

$$U_{90\%\ CI,PCT} = k \cdot \sqrt{\left(SD_{i,pooled,R-AP-107}\right)^2 + \left(SD_{i,pooled,S-AP-107}\right)^2} \tag{4.1}$$

where: $SD_{i,pooled,R\text{-}AP\text{-}107}$ = pooled standard deviation of element i for ln[NL_i, g·m^{-2}] for R-AP-107
$SD_{i,pooled,S\text{-}AP\text{-}107}$ = pooled standard deviation of element i for ln[NL_i, g·m^{-2}] for S-AP-107
k = 1.64485 = error multiplier for a 90% confidence interval

Figure 4.1b shows a plot of the absolute value of the differences of average ln[NL_i, g·m^{-2}] between R-AP-107 and S-AP-107 for B and Na where the error bars represent $U_{90\%\ CI,\ PCT}$. Since the error bars cross the zero line for B and Na, the differences are not statistically significant (i.e., differences are within measurement error).

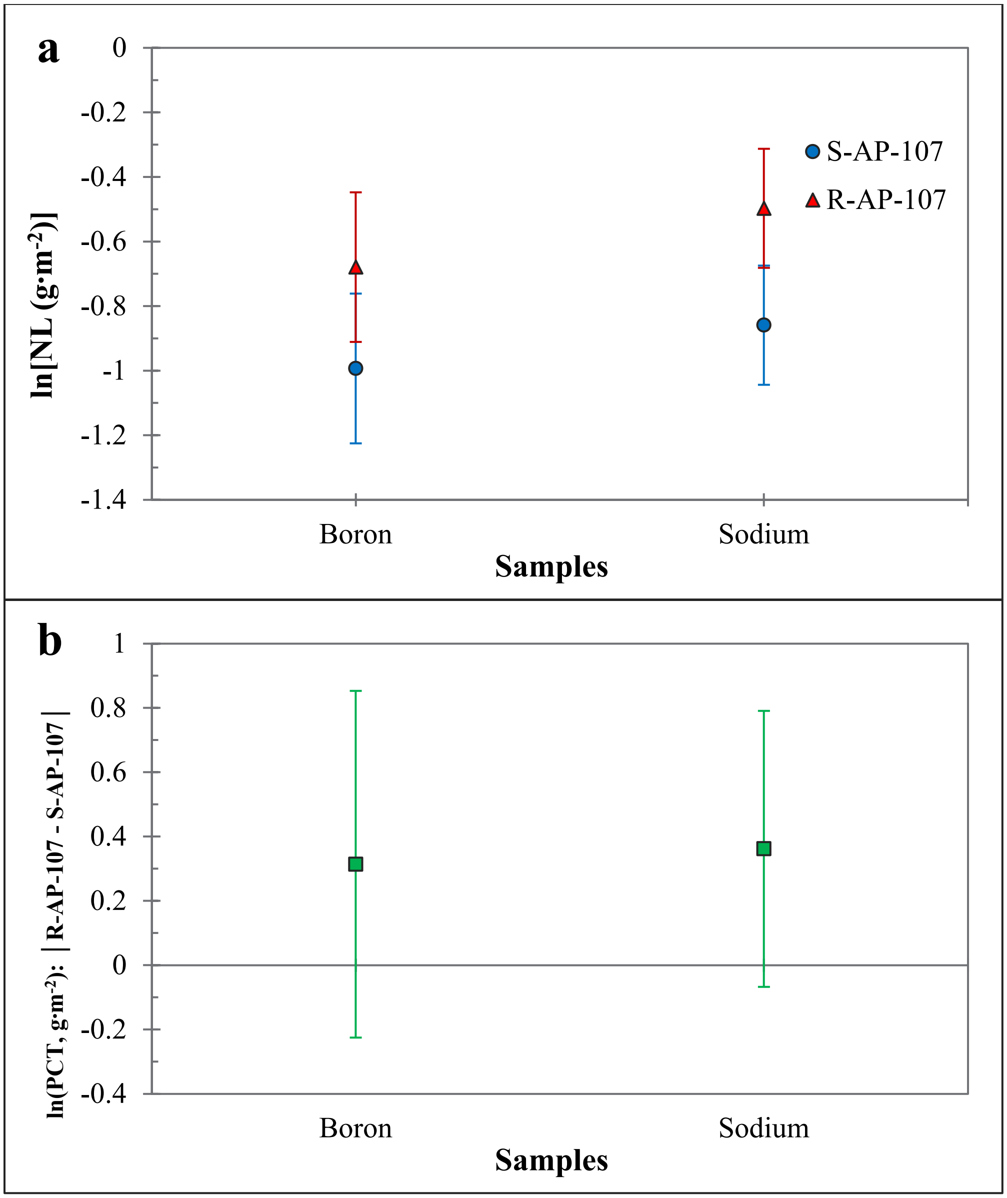

Figure 4.1. a) average ln[NL_i, g·m^2] boron and sodium responses for S-AP-107 and R-AP-107. Uncertainty is represented by $SD_{i,pooled}$ values from Vienna et al. (2022). b) differences of S-AP-107 and R-AP-107 average ln(NL_i, g·m^2) boron and sodium responses respectively. Uncertainties are associated with 90% confidence intervals ($U_{90\%\ CI,\ PCT}$) as described in Equation 4.1.

Finally, an approximate z-statistic (Z_{PCT}) was calculated for the differences between the R-AP-107 and S-AP-107 ln[NL_i, g·m^2] results for B and Na using $SD_{i,pooled}$ values via Equation 4.2:

$$Z_{PCT} = \frac{|\ln[NL_i]_{R-AP-107} - \ln[NL_i]_{S-AP-107}|}{\sqrt{\left(SD_{i,pooled,R-AP-107}\right)^2 + \left(SD_{i,pooled,S-AP-107}\right)^2}} \tag{4.2}$$

where: $\ln[NL_i]_{R-AP-107}$ = ln[NL_i, g·m^{-2}] for R-AP-107

$\ln[NL_i]_{S-AP-107}$ = ln[NL_i, g·m^{-2}] for S-AP-107

$SD_{i,pooled}$ = uncertainty of ln[NL_i, g·m^{-2}] for R-AP-107

$SD_{i,pooled}$ = uncertainty of ln[NL_i, g·m^{-2}] for S-AP-107

Table 4.5 shows the Z_{PCT} and *P-values* determined for the differences between the R-AP-107 and S-AP-107 average ln[NL_i, g·m^{-2}] results for boron and sodium. The p-values comparing the differences for ln[NR_B, g·m^{-2}] and ln[NR_{Na}, g·m^{-2}] between R-AP-107 and S-AP-107 were all well above the commonly used thresholds for significant differences of 0.05 or 0.10, suggesting the differences in ln[NR_B, g·m$^{-2]}$ and ln[NR_{Na}, g·m^{-2}] between R-AP-107 and S-AP-107 are within measurement uncertainties.

Table 4.5. Z_{PCT} and *P-values* determined for the differences between the R-AP-107 and S-AP-107 ln[NL_i, g·m^2] results for boron and sodium.

Result	Boron	Sodium
Z_{PCT}	0.9585	1.3873
P-value	0.3378	0.1654

All statistical comparisons employed for the PCT results indicate that the R-AP-107 and S-AP-107 responses are within experimental uncertainty for both boron and sodium.

4.2 Vapor Hydration Test

4.2.1 VHT Results

Table 4.6 presents pH_{RT}, evaporation observations, VHT corrosion rates (r_{VHT}, g m^{-2} d^{-1}), propagated error for r_{VHT} ($\sigma_{r_{prop}}$), ln[r_{VHT}, g m^{-2} d^{-1}], and propagated error for ln[r_{VHT}] ($\sigma_{ln(r_{prop})}$) for individual R-AP-107 and S-AP-107 VHT experiments. The pH_{RT} was not determined for three experiments because not enough solution was present for a pH_{RT} measurement. For the experiments that pH_{RT} was measured, the pH_{RT} values were <10 indicating that refluxing conditions were not present. The experiments with >50% solution loss over the duration of the experiments are considered invalid per ASTM C1663-18. The invalid experiments were not repeated due to the high cost and effort required to redo the tests especially when other replicate tests were valid.

Including the tests that lost >50% solution, all the rates are within uncertainty and the r_{VHT} values range from -1 ± 3 g m^{-2} d^{-1} to 4 ± 7 g m^{-2} d^{-1}. All samples appeared unaltered during post-experiment analysis as seen in Figure 3.2. Any changes in glass thickness before and after VHT experiments are attributed to variances in thickness across the sample that were not captured with calipers before the experiments rather than glass alteration. The thicknesses of the coupons were not uniform due to polishing complications with samples mounted on the aluminum puck.

In accordance with the WTP contract, the VHT corrosion rates (r_{VHT}) of LAW glasses subjected to >7-day VHT shall be less than 50 g m^{-2} d^{-1} (DOE 2000). All experiments recorded r_{VHT} < 50 g m^{-2} d^{-1} indicating the results satisfy the contract requirement.

Table 4.6. Individual pH_{RT}, evaporation observations, VHT corrosion rates (r_{VHT}, g m^{-2} d^{-1}), propagated error for r_{VHT} ($\sigma_{r_{prop}}$), ln[r_{VHT}, g m^{-2} d^{-1}], and propagated error for ln[r_{VHT}] ($\sigma_{ln(r_{prop})}$) for R-AP-107 and S-AP-107. Not detected results are represented by "ND". Not applicable results are represented by "NA".

Sample ID	pH_{RT}	Did the experiment lose >50% solution?	r_{VHT} (g·m^{-2}·d^{-1})	$\sigma_{r_{prop}}$ (g·m^{-2}·d^{-1})	$\ln[r_{VHT}$, g·m^{-2}·d$^{-1}]$	$\sigma_{ln(r_{prop})}$
R-AP-107-VHT-A	ND	yes	3	5	1.1	1.6
R-AP-107-VHT-B	ND	yes	2	4	0.5	2.6
R-AP-107-VHT-C	7	no	4	7	1.3	1.8
S-AP-107-VHT-A	ND	yes	-1	3	NA	NA
S-AP-107-VHT-B	7	no	0	3	-1.5	11.5
S-AP-107-VHT-C	7	no	3	8	1.2	2.5

Average ln[r_{VHT}] ($\overline{\ln[r_{VHT}]}$), standard deviations for $\overline{\ln[r_{VHT}]}$ ($SD_{\ln[r_{VHT}]}$), and propagated error for $\overline{\ln[r_{VHT}]}$ ($\bar{\sigma}_{\ln[r_{prop}]}$) for R-AP-107 and S-AP-107 were calculated using all samples and using samples with <50% evaporation loss. Results are shown in Table 4.7. No $SD_{\ln[r_{VHT}]}$ was calculated for the R-AP-107 samples with <50% evaporation loss as R-AP-107-VHT-c was the only R-AP-107 replicate that satisfied the requirement.

Table 4.7. Average ln[r_{VHT}, g·m^{-2}·d] ($\overline{\ln[r_{VHT}]}$), standard deviations for $\overline{\ln[r_{VHT}]}$ ($SD_{\ln[r_{VHT}]}$), and propagated error for $\overline{\ln[r_{VHT}]}$ ($\bar{\sigma}_{\ln[r_{prop}]}$) for R-AP-107 and S-AP-107 for all samples and samples with <50% evaporation loss. Not applicable results are represented by "NA".

Category	Sample ID	$\overline{\ln[r_{VHT}]}$	$SD_{\ln[r_{VHT}]}$	$\bar{\sigma}_{\ln[r_{prop}]}$
All Samples	R-AP-107	1.0	0.4	1.2
	S-AP-107	-0.2*	1.9	5.9*
Samples with <50% evaporation loss	R-AP-107	1.3	NA	1.8
	S-AP-107	-0.2	1.9	5.9

*S-AP-107-VHT-A results are excluded since the individual values are "NA"

4.2.2 VHT Statistical Comparisons

When uncertainties were propagated from individual remaining thickness measurement uncertainties, all individual r_{VHT} values were within uncertainty. However, statistical analysis was still performed on the VHT samples to evaluate whether the average ln[r_{VHT} g·m^{-2}·d^{-1}] responses ($\overline{\ln[r_{VHT}]}$) of R-AP-107 and S-AP-107 were within experimental uncertainty of each other when various approaches to calculating uncertainties were employed.

Thus, statistical analysis comparisons were performed on $\overline{\ln[r_{VHT}]}$ for all samples and samples with <50% evaporation loss for R-AP-107 and S-AP-107. Uncertainties for $\overline{\ln[r_{VHT}]}$ used in the statistical analyses were determined using errors from multiple approaches including 1) $SD_{\ln[r_{VHT}]}$, 2) $\bar{\sigma}_{\ln[r_{prop}]}$, and 3) a pooled standard deviation for ln($r_{VHT,}$ g·m^{-2}·d^{-1}) ($SD_{VHT,pooled}$). The $\overline{\ln[r_{VHT}]}$, $SD_{\ln[r_{VHT}]}$, and $\bar{\sigma}_{\ln[r_{prop}]}$ values are provided in Table 4.7. The $SD_{VHT,pooled}$ is 0.9034 for the general non-rad LAW glass ln($r_{VHT,}$ g·m^{-2}·d^{-1}) results and includes uncertainties due to fabricating glasses, performing VHTs, and sample analysis.

Figure 4.2 shows the $\overline{\ln[r_{VHT}]}$ responses for R-AP-107 and S-AP-107 determined for all samples and samples with <50% evaporation loss where the error bars represent a) $SD_{\ln[r_{VHT}]}$, b) $\bar{\sigma}_{\ln[r_{prop}]}$, and c) $SD_{VHT,pooled}$. The R-AP-107 and S-AP-107 $\overline{\ln[r_{VHT}]}$ values are within uncertainty regardless of the error method employed.

Further statistical analysis was performed to evaluate the absolute values of the differences of $\overline{\ln[r_{VHT}]}$ between R-AP-107 and S-AP-107 to see if the differences were greater than zero within the 90% confidence interval uncertainty for all samples and only the samples with <50% evaporation loss. The 90% confidence interval uncertainty for VHT ($U_{90\%\ CI,\ VHT}$) was calculated using Equation 4.3:

$$U_{90\%\ CI,VHT} = k \cdot \sqrt{\left(u_{\ln(r_{VHT}),R-AP-107}\right)^2 + \left(u_{\ln(r_{VHT}),S-AP-107}\right)^2} \tag{4.3}$$

where: $u_{\ln(r_{VHT}),R-AP-107}$ = uncertainty of $\overline{\ln[r_{VHT}]}$ for R-AP-107
$u_{\ln(r_{VHT}),S-AP-107}$ = uncertainty of $\overline{\ln[r_{VHT}]}$ for S-AP-107
k = 1.64485 = error multiplier (z multiplier for a 90% confidence interval).

The $U_{90\%\ CI,\ VHT}$ values were determined via Equation 4.3 using $\bar{\sigma}_{\ln[r_{prop}]}$ and $SD_{VHT,pooled}$ values as uncertainties; however, a slight variant of Equation 4.3 was used when $U_{90\%\ CI,\ VHT}$ was determined from $SD_{\ln[r_{VHT}]}$ (i.e., $U_{90\%\ CI,\ VHT\text{-}SD}$) since the sample size was no longer considered large (i.e., t-statistic conditions apply rather than approximate z-test conditions). Therefore, Equation 4.4 was used to determine $U_{90\%\ CI,\ VHT\text{-}SD}$:

$$U_{90\%\ CI,VHT-SD} = k \cdot \sqrt{\frac{\left(SD_{\ln[r_{VHT}],R-AP-107}\right)^2}{p} + \frac{\left(SD_{\ln[r_{VHT}],S-AP-107}\right)^2}{q}} \tag{4.4}$$

where: p = number of R-AP-107 tests
q = number of S-AP-107 tests
k = 6.31375 = error multiplier (t multiplier based for a 90% confidence interval for these tests).

Figure 4.3 shows a plot of the absolute value of the differences of $\overline{\ln[r_{VHT}]}$ between R-AP-107 and S-AP-107 for all samples and for samples with <50% evaporation loss where the error bars represent $u_{90\%\ CI,VHT}$ determined from a) $SD_{\ln[r_{VHT}]}$, b) $\bar{\sigma}_{\ln[r_{prop}]}$, and c) $SD_{VHT,pooled}$. Since the error bars cross the zero line for all samples and samples with <50% evaporation loss in all cases (except when $SD_{\ln[r_{VHT}]}$ was used to determine $u_{90\%\ CI,\ VHT\text{-}SD}$ for samples with <50% evaporation loss as no $SD_{\ln[r_{VHT}]}$ was calculated for R-AP-107), the differences are not statistically significant (i.e., differences are within measurement error).

The various approaches to determine uncertainty highlight the major source of error within these VHTs. Since $SD_{VHT,pooled}$ is determined from a large data set (i.e., 77 degrees of freedom), it is expected to have the largest error as it is the most representative estimate of the true VHT error. However, $SD_{\ln[r_{VHT}]}$ for S-AP-107 for both scenarios and $\bar{\sigma}_{\ln[r_{prop}]}$ for all scenarios for R-AP-107 and S-AP-107 are larger (where $\bar{\sigma}_{\ln[r_{prop}]}$ is considerably larger) than $SD_{VHT,pooled}$. The $SD_{\ln[r_{VHT}]}$ and $\bar{\sigma}_{\ln[r_{prop}]}$ were calculated specifically for the R-AP-107 and S-AP-107 samples and capture experimental uncertainties in the thickness measurements derived from the modified polishing procedure and the thickness measurement methods. The samples used to determine $SD_{VHT,pooled}$ were polished according to the polishing procedure described in ASTM C1663-18, which does not lead to as extreme variation in thickness across the coupons. Therefore, $SD_{VHT,pooled}$ is not the most representative of total experimental uncertainty for these particular samples.

Uncertainities associated with $SD_{\ln[r_{VHT}]}$

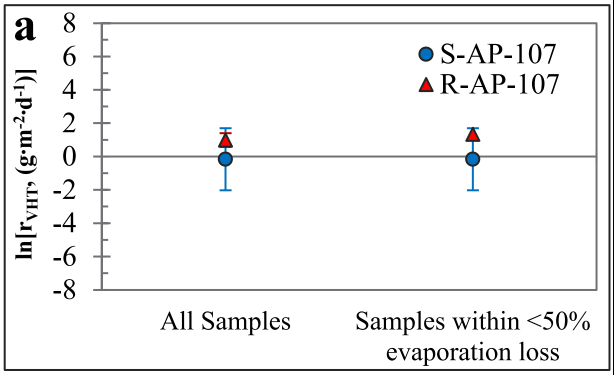

Uncertainities associated with $\bar{\sigma}_{\ln[r_{prop}]}$

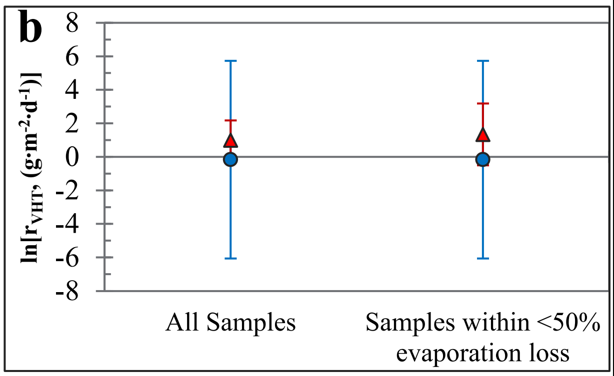

Uncertainities associated with $SD_{VHT,pooled}$

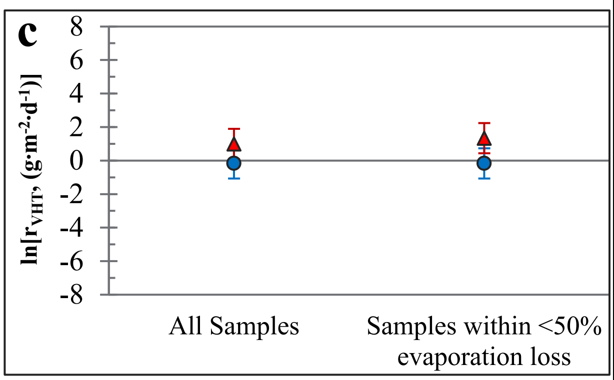

Figure 4.2. Average ln[r_{VHT}, g·m^2] responses (i.e., $\overline{\ln[r_{VHT}]}$) for S-AP-107 and R-AP-107 determined for all samples and samples with <50% evaporation loss where uncertainty is represented by a) $SD_{\ln[r_{VHT}]}$, b) $\bar{\sigma}_{\ln[r_{prop}]}$, and c) $SD_{VHT,pooled}$.

Uncertainities associated with $SD_{\ln[r_{VHT}]}$

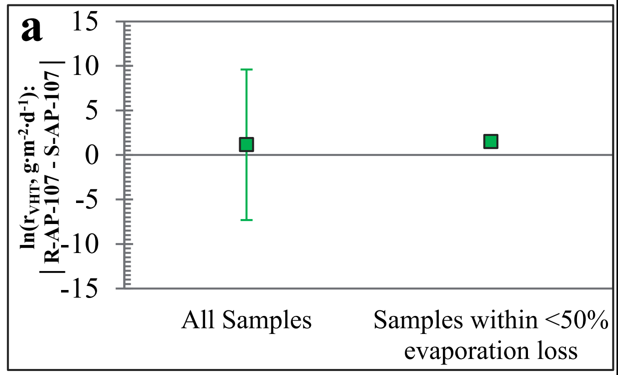

Uncertainities associated with $\bar{\sigma}_{\ln[r_{prop}]}$

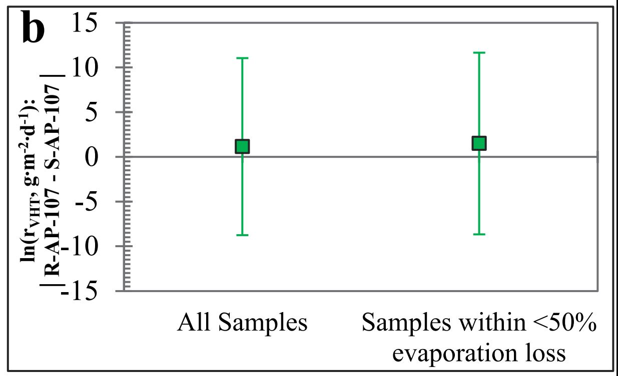

Uncertainities associated with $SD_{VHT,pooled}$

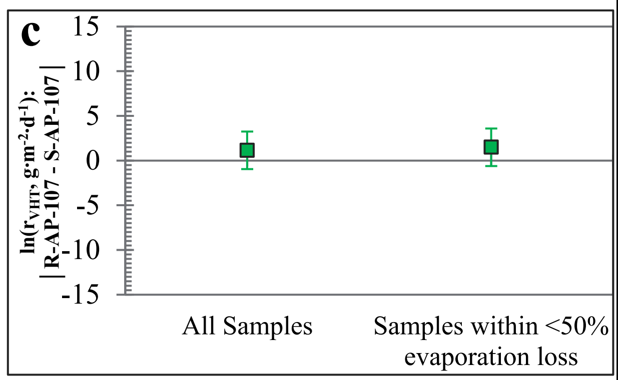

Figure 4.3. Differences of S-AP-107 and R-AP-average ln[r_{VHT}, g·m^2] responses (i.e., $\overline{\ln[r_{VHT}]}$) for all samples and samples with <50% evaporation loss are shown where uncertainties are associated with 90% confidence intervals ($U_{90\%\ CI,VHT}$) determined from a) $SD_{\ln[r_{VHT}]}$, b) $\bar{\sigma}_{\ln[r_{prop}]}$, and c) $SD_{VHT,pooled}$ as described in Equations 4.2 and 4.3.

Finally, test statistics were calculated for the differences between the R-AP-107 and S-AP-107 $\overline{\ln[r_{VHT}]}$ results for all samples and samples with <50% evaporation loss using $SD_{\ln[r_{VHT}]}$, $\bar{\sigma}_{\ln[r_{prop}]}$, and $SD_{VHT,pooled}$ as uncertainties. When $SD_{\ln[r_{VHT}]}$ was used to represent errors, a t-statistic (T_{VHT}) was determined because the sample population was considered small. The equation for the t-statistic is given by Equation 4.5:

$$T_{VHT} = \frac{\left|\overline{\ln[r_{VHT}]}_{R-AP-107} - \overline{\ln[r_{VHT}]}_{S-AP-107}\right|}{\sqrt{\frac{\left(SD_{\ln[r_{VHT}],R-AP-107}\right)^2}{p} + \frac{\left(SD_{\ln[r_{VHT}],S-AP-107}\right)^2}{q}}} \tag{4.5}$$

where: p = number of R-AP-107 tests
q = number of S-AP-107 tests.

When $\bar{\sigma}_{\ln[r_{prop}]}$ and $SD_{VHT,pooled}$ were used as uncertainties, an approximate z-statistic was calculated as the sample population was considered large. The general z-statistic equation for VHT results (Z_{VHT}) is given in Equation 4.6:

$$Z_{VHT} = \frac{\left|\overline{\ln[r_{VHT}]}_{R-AP-107} - \overline{\ln[r_{VHT}]}_{S-AP-107}\right|}{\sqrt{\left(\mu_{\ln(NL_i),R-AP-107}\right)^2 + \left(\mu_{\ln(NL_i),S-AP-107}\right)^2}} \tag{4.6}$$

where: $\mu_{\ln(r_{VHT}),R-AP-107}$ = uncertainty of $\overline{\ln[r_{VHT}]}$ for R-AP-107
$\mu_{\ln(r_{VHT}),S-AP-107}$ = uncertainty of $\overline{\ln[r_{VHT}]}$ for S-AP-107

Table 4.8 shows the test statistics (T_{VHT} and Z_{VHT}) and *P-values* determined for the differences between the R-AP-107 and S-AP-107 $\overline{\ln[r_{VHT}]}$ results determined for all samples and samples with <50% evaporation loss with uncertainties represented by $SD_{\ln[r_{VHT}]}$, $\bar{\sigma}_{\ln[r_{prop}]}$, and $SD_{VHT,pooled}$, respectively. In every case where they could be calculated, the *P-values* comparing the differences between R-AP-107 and S-AP-107 were all well above the commonly used thresholds for significant differences of 0.05 or 0.10, suggesting the differences in $\overline{\ln[r_{VHT}]}$ between R-AP-107 and S-AP-107 are within measurement uncertainties.

Table 4.8. Statistical tests (T_{VHT} and-Z_{VHT}) and *P-values* determined for the differences between the R-AP-107 and S-AP-107 $\overline{\ln[r_{VHT}]}$ results for all samples and samples <50% evaporation loss.

Uncertainty Source	**Result**	**All Samples**	**Samples <50% evaporation loss**
$SD_{\ln[r_{VHT}]}$	T_{VHT}	0.8618	NA
	P-value	0.5472	NA
$\bar{\sigma}_{\ln[r_{prop}]}$	Z_{VHT}	0.1918	0.2430
	P-value	0.8479	0.8080
$SD_{VHT,pooled}$	Z_{VHT}	0.9034	1.1759
	P-value	0.3663	0.2396

All statistical comparisons employed for the VHT results indicate that the R-AP-107 and S-AP-107 responses are within experimental uncertainty regardless of the uncertainty calculation method or whether all samples or samples with <50% evaporation loss were considered.

5.0 Conclusions

PCT and VHT experiments were conducted on radioactive waste glass (R-AP-107) and non-radioactive simulant glass (S-AP-107) to determine whether their PCT and VHT responses are significantly different. The glasses were prepared identically and tested side by side to reduce experimental uncertainties caused by differences in equipment and protocols.

The PCT results and statistical analyses of the results are presented in Section 3.1:

- The average NL_B (g·m^{-2}) values and standard deviations were (0.51 ± 0.09) g·m^{-2} and (0.37 ± 0.01) g·m^{-2} for R-AP-107 and S-AP-107, respectively.
- The average NL_{Na} values were (0.61 ± 0.04) g·m^{-2} and (0.42 ± 0.01) g·m^{-2} for R-AP-107 and S-AP-107, respectively.
- Average NL_{Tc} was measured for R-AP-107 to be 0.58 g·m^{-2} which is consistent with the R-AP-107 NL_B and NL_{Na} values.

In general, the slightly higher PCT responses for R-AP-107 were attributed to the 61 RPD higher concentrations of Li_2O in the R-AP-107 glass. However, statistical analyses (i.e., difference comparisons, z-statistics, p-values) using previously determined pooled SD values ($SD_{i,pooled}$) indicated that the ln[NL_i] values of R-AP-107 and S-AP-107 were within experimental error even with the glass compositional differences.

The VHT results and statistical analyses of the results are presented in Section 4.2. The r_{VHT} (g·m^{-2}·d^{-1}) values ranged from -1 to 4 g·m^{-2}·d^{-1} and were all within uncertainty. No alteration was detected during post experimental analysis. Statistical analyses (i.e., difference comparisons, t-statistics/z-statistics, p-values) were performed using uncertainties determined from three approaches: 1) standard deviations of the replicate tests, 2) errors propagated from the uncertainties associated with individual remaining thickness measurements, and 3) a pooled SD value. The R-AP-107 and S-AP-107 ln[r_{VHT}] results were within experimental uncertainty of each other regardless of which uncertainty approach was taken and whether all six samples or only the three samples with <50% evaporation loss were considered. The uncertainties derived from error propagation of individual thickness measurements were considerably larger than the other uncertainties where the largest source of experimental error was identified to be from thickness variations across the coupons that were not adequately captured by calipers. The thickness variations were due to modifications of the polishing procedure for safety reasons.

6.0 Bibliography

ASTM C1285-21, *Standard Test Methods for Determining Chemical Durability of Nuclear, Hazardous, and Mixed Waste Glasses and Multiphase Glass Ceramics: The Product Consistency Test (PCT)*. ASTM International, West Conshohocken, Pennsylvania.

ASTM C1663-18, *Standard Test Method for Measuring Waste Glass or Glass Ceramic Durability by Vapor Hydration Test*. ASTM International, West Conshohocken, Pennsylvania.

ASTM D1193-06R18, *Standard Specification for Reagent Water*. ASTM International, West Conshohocken, Pennsylvania.

Bernards GA, GA Hersi, TM Hohl, RT Jasper, PD Mahoney, NK Pak, SD Reaksecker, AJ Schubick, and EB West. 2020. *River Protection Project System Plan*. ORP-11242, Rev. 9, U.S. Department of Energy, Office of River Protection, Richland, Washington.

Bibler. NE, AR Jurgensen. 1987. *Leaching Tc-99 form SRP Glass in simulated Tuff and Salt Groundwaters.* DP-MS-87-70, Savannah River National Laboratory, Aiken, South Carolina.

Crawford CL, DM Ferrara, RF Schumacher, and NE Bibler. 2000. *Crucible-Scale Active Vitrification Testing Envelope C, Tank 241-an-102 (U)*, WSRC-TR-2000-00371, Rev. 0, Westinghouse Savannah River Company, Aiken, SC.

DOE. 2000. *Design, Construction, and Commissioning of the Hanford Tank Waste Treatment and Immobilization Plant*. Contract DE-AC27-01RV14136, as amended, U.S. Department of Energy, Office of River Protection, Richland, Washington.

Dixon DR, Westesen AM, Hall MA, Stewart CM, Lang JB, Cutforth DA, Eaton WC, Peterson RA. *Vitrification of Hanford Tank 241-AP-107 with Recycled Condensate*. RPT-DFTP-024, Rev 0. Richland, WA (United States): 2020. DOI: 10.2172/1766813.

Ebert WL. 2019. *The Precision of Product Consistency Tests with Reference Glasses ARM-1 and SRM 623*. ANL/CFCT-19/29, Argonne National Laboratory, Argonne, Illinois.

Kim DS and JD Vienna. 2012. *Preliminary ILAW Formulation Algorithm Description*. 24590 LAW-RPT-RT-04-0003, Rev. 1, River Protection Project, Hanford Waste Treatment and Immobilization Plant, Richland, Washington.

Muller, IS, B Dutta, CF Feng, F Perez-cardenas, H Gan, IL Pegg, K Hight, M Laurenzi, S Grant, T Shatz, B Bitner, C Mooers, E Malone, G Bazemore, I Carranza, J Berger, L Su, M Timmons, ST Lai. 2001. *Final Report: Glass Formulation And Testing With RPP-WTP LAW Simulants.* VSL-01R3560-2, Rev. 0. Vitreous State Laboratory, The Catholic University of America, Washington, D.C.

NQA-1-2012, *Quality Assurance Requirements for Nuclear Facility Application.* American Society of Mechanical Engineers, New York, New York.

Piepel GF, SK Cooley, IS Muller, H Gan, I Joseph, and IL Pegg. 2007. *ILAW PCT, VHT, Viscosity, and Electrical Conductivity Model Development*. VSL-07R1230-1, Rev. 0, ORP-56502, Vitreous State Laboratory, The Catholic University of America, Washington, D.C.

Rielley, E, CF Feng, E Kashnikov, H Gan, IS Muller, J Singh, L Goloski, N D'Angelo, S Grant, S Watts, Y Liu, C Boice, C Mooers, G Bazemore, IL Pegg, J Cheron, KD Derr, L Su, R Cecil, ST Lai, T Moncrief. 2001. *Final Report: Preparation and Testing of Law Matrix Glasses*. VSL-04R4480-1, Rev. 0. Vitreous State Laboratory, The Catholic University of America, Washington, D.C.

Vienna JD, P Hrma, A Jiricka, DE Smith, TH Lorier, IA Reamer, and RL Schultz. 2001. *Hanford Immobilized LAW Product Acceptance Testing: Tanks Focus Area Results*. PNNL-13744, Pacific Northwest National Laboratory, Richland, Washington.

Vienna, J.D. 2004. "Contract Requirement for ILAW Qualification Testing," to C.A. Musick, CCN: 089927, May 14, 2004, River Protection Project, Waste Treatment Plant, Richland, WA.

Vienna JD, A Heredia-Langner, SK Cooley, AE Holmes, DS Kim, and NA Lumetta. 2022. *Glass Property-Composition Models for Support of Hanford WTP LAW Facility Operation*. PNNL-30932, Rev. 2, Pacific Northwest National Laboratory, Richland, Washington.

WADOE, *Hanford Facility Resource Conservation and Recovery Act (RCRA) Permit for the Treatment, Storage, and Disposal of Dangerous Waste*, Part III, Operating Unit Group 10 (WA7890008967), Waste Treatment and Immobilization Plant. Washington State Department of Ecology, Olympia, WA.

Appendix A – Glass Compositions for PCTs

Table A.1 Measured composition of ARM-1 from Ebert (2019).

	Measured, oxide mass fraction
Component	**ARM-1**
Al_2O_3	0.0559
B_2O_3	0.113
BaO	0.0066
CaO	0.0224
CeO_2	0.0151
Cs_2O	0.0117
Li_2O	0.0508
MoO_3	0.0166
Na_2O	0.0966
Nd_2O_3	0.0596
SiO_2	0.465
SrO	0.0045
TiO_2	0.0321
ZnO	0.0146
ZrO_2	0.018
P_2O_5	0.0065

Table A.2 Measured elemental weight fractions of R-AP-107, S-AP-107, and ARM-1 used for PCT calculations (i.e., NC_i and NL_i).

	S-AP-107	R-AP-107	ARM-1
Al	3.07E-02	3.14E-02	2.96E-02
B	3.00E-02	3.01E-02	3.51E-02
Ba	1.12E-04	3.77E-05	5.91E-03
Ca	2.56E-02	3.16E-02	1.60E-02
Cd	6.32E-06	4.75E-06	0.00E+00
Ce	0.00E+00	0.00E+00	1.23E-02
Cr	8.37E-04	8.85E-04	0.00E+00
Cs	0.00E+00	4.03E-06	1.10E-02
Co	7.03E-06	3.80E-06	0.00E+00
Cu	1.72E-05	1.81E-05	0.00E+00
Fe	4.17E-02	3.71E-02	0.00E+00
K	3.11E-03	3.10E-03	0.00E+00
La	5.75E-04	2.51E-06	0.00E+00
Pb	3.22E-05	5.01E-06	0.00E+00
Li	3.48E-03	6.52E-03	2.36E-02
Mg	8.68E-03	8.55E-03	0.00E+00
Mn	9.82E-05	8.77E-05	0.00E+00
Mo	2.05E-04	4.77E-05	1.11E-02
Na	1.25E-01	1.25E-01	7.17E-02
Nd	0.00E+00	0.00E+00	5.11E-02
Ni	3.23E-04	1.63E-04	0.00E+00
Si	2.15E-01	2.13E-01	2.17E-01
Sr	8.73E-05	3.65E-05	3.81E-03
Tc	0.00E+00	2.24E-06	0.00E+00
Ti	8.86E-03	8.41E-03	1.92E-02
Zn	2.72E-02	2.84E-02	1.17E-02
Zr	2.03E-02	2.04E-02	1.33E-02
Cl	2.44E-03	0.00E+00	0.00E+00
F	1.42E-04	4.34E-04	0.00E+00
P	7.42E-04	6.28E-04	2.84E-03
S	1.69E-03	1.57E-03	0.00E+00
Sn	1.80E-05	2.43E-05	0.00E+00
Re	4.37E-06	0.00E+00	0.00E+00
U	0.00E+00	0.00E+00	0.00E+00
W	1.96E-04	2.47E-04	0.00E+00
V	6.01E-05	5.44E-05	0.00E+00
Y	4.15E-05	3.93E-05	0.00E+00

Appendix B – VHT coupon dimensions

Table B.1 Initial glass dimension average measurements (w_i, l_i, d_i; mm) before VHT experiments. Uncertainties are expressed as standard deviations of the three measurements in each dimension.

Measurement	R-AP-107-VHT-a	R-AP-107-VHT-b	R-AP-107-VHT-c	S-AP-107-VHT-a	S-AP-107-VHT-b	S-AP-107-VHT c
w_i	9.11 ± 0.03	9.47 ± 0.03	9.73 ± 0.02	8.80 ± 0.06	8.95 ± 0.05	8.99 ± 0.06
l_i	10.20 ± 0.03	9.81 ± 0.02	10.05 ± 0.05	10.01 ± 0.04	9.42 ± 0.03	10.36 ± 0.05
d_i	1.67 ± 0.04	1.76 ± 0.04	1.75 ± 0.06	1.62 ± 0.05	1.71 ± 0.02	1.53 ± 0.05

Table B.2 Remaining glass thickness measurements (d_r, mm) after VHT experiments

Measurement	R-AP-107-VHT-a	R-AP-107-VHT-b	R-AP-107-VHT-c	S-AP-107-VHT-a	S-AP-107-VHT-b	S-AP-107-VHT c
1	1.409	1.580	1.414	1.672	1.726	1.210
2	1.546	1.661	1.553	1.672	1.739	1.299
3	1.611	1.719	1.684	1.666	1.739	1.376
4	1.657	1.761	1.752	1.661	1.737	1.438
5	1.675	1.790	1.781	1.651	1.737	1.493
6	1.688	1.803	1.794	1.637	1.737	1.538
7	1.679	1.799	1.779	1.626	1.712	1.566
8	1.668	1.783	1.743	1.611	1.690	1.595
9	1.633	1.752	1.686	1.584	1.657	1.602
10	1.582	1.701	1.582	1.560	1.619	1.573
Average	**1.61**	**1.73**	**1.7**	**1.63**	**1.71**	**1.5**
SD	**0.09**	**0.07**	**0.1**	**0.04**	**0.04**	**0.1**